

Spectrum Sensing Under Hardware Constraints

Alexandros – Apostolos A. Boulogeorgos, *Student Member, IEEE*, Nestor D.

Chatzidiamantis, *Member, IEEE*, and George K. Karagiannidis, *Fellow, IEEE*

Abstract

Direct-conversion radio (DCR) receivers can offer highly integrated low-cost hardware solutions for spectrum sensing in cognitive radio systems. However, DCR receivers are susceptible to radio frequency (RF) impairments, such as in-phase and quadrature-phase imbalance, low-noise amplifier nonlinearities and phase noise, which limit the spectrum sensing capabilities. In this paper, we investigate the joint effects of RF impairments on energy detection based spectrum sensing for cognitive radio (CR) systems in multi-channel environments. In particular, we provide closed-form expressions for the evaluation of the detection and false alarm probabilities, assuming Rayleigh fading. Furthermore, we extend the analysis to the case of CR networks with cooperative sensing, where the secondary users suffer from different levels of RF imperfections, considering both scenarios of error free and imperfect reporting channel. Numerical and simulation results demonstrate the accuracy of the analysis as well as the detrimental effects of RF imperfections on the spectrum sensing performance, which bring significant losses in the spectrum utilization.

Index Terms

Cognitive radio, Cooperative sensing, Detection probability, Direct-conversion receivers, Energy

This work was presented in part at IEEE ICC 2015 - Seventh Workshop on Cooperative and Cognitive Networks (CoCoNet7).

A.-A. A. Boulogeorgos, N. D. Chatzidiamantis and G. K. Karagiannidis are with the Department of Electrical and Computer Engineering, Aristotle University of Thessaloniki, 54 124, Thessaloniki, Greece (e-mail: {ampoulog, nestoras, geokarag}@auth.gr).

detectors, Fading channels, False alarm probability, Hardware constraints, I/Q imbalance, LNA nonlinearities, Phase noise, Receiver operation curves, RF imperfections, Wideband sensing.

I. INTRODUCTION

The rapid growth of wireless communications and the foreseen spectrum occupancy problems, due to the exponentially increasing consumer demands on mobile traffic and data, motivated the evolution of the concept of cognitive radio (CR) [1]. CR systems require intelligent reconfigurable wireless devices, capable of sensing the conditions of the surrounding radio frequency (RF) environment and modifying their transmission parameters accordingly, in order to achieve the best overall performance, without interfering with other users [2]. One fundamental task in CR is spectrum sensing, i.e., the identification of temporarily vacant portions of spectrum, over wide ranges of spectrum resources and determine the available spectrum holes on its own. Spectrum sensing allows the exploitation of the under-utilized spectrum, which is considered to be an essential element in the operation of CRs. Therefore, great amount of effort has been put to derive optimal, suboptimal, ad-hoc, and cooperative solutions to the spectrum sensing problem (see for example [3]–[13]). However, the majority of these works ignore the imperfections associated with the RF front-end. Such imperfections, which are encountered in the widely deployed low-cost direct-conversion radio (DCR) receivers (RXs), include in-phase (I) and quadrature-phase (Q) imbalance (IQI) [14], low-noise amplifier (LNA) nonlinearities [15] and phase noise (PHN) [16].

The effects of RF imperfections in general were studied in several works [16]–[35]. However, only recently, the impacts of RF imperfections in the spectrum sensing capabilities of CR was investigated [14], [16], [21], [22], [32]–[35]. In particular, the importance of improved front-end linearity and sensitivity was illustrated in [32] and [33], while the impacts of RF impairments in DCRs on single-channel energy and/or cyclostationary based sensing were discussed in [21] and [22]. Furthermore, in [34] the authors presented closed-form expressions for the detection and false alarm probabilities for the Neyman-Pearson detector, considering the spectrum sensing

problem in single-channel orthogonal frequency division multiplexing (OFDM) CR RX, under the joint effect of transmitter and receiver IQI. On the other hand, multi-channel sensing under IQI was reported in [35], where a three-level hypothesis blind detector was introduced. Moreover, the impact of RF IQI on energy detection (ED) for both single-channel and multi-channel DCRs was investigated in [14], where it was shown that the false alarm probability in a multi-channel environment increases significantly, compared to the ideal RF RX case. Additionally, in [16], the authors analyzed the effect of PHN on ED, considering a multi-channel DCR and additive white Gaussian noise (AWGN) channels, whereas in [36], the impact of third-order non-linearities on the detection and false alarm probabilities for classical and cyclostationary energy detectors considering imperfect LNA, was investigated.

In this work, we investigate the impact on the multi-channel energy-based spectrum sensing mechanism of the joint effects of several RF impairments, such as LNA non-linearities, PHN and IQI. After assuming flat-fading Rayleigh channels and complex Gaussian primary user (PU) transmitted signals, and approximating the joint effects of RF impairments by a complex Gaussian process (an approximation which has been validated both in theory and by experiments, see [25] and the references therein), we derive closed-form expressions for the probabilities of false alarm and detection. Based on these expressions, we investigate the impact of RF impairments on ED. Specifically, the contribution of this paper can be summarized as follows:

- We, first, derive analytical closed-form expressions for the false alarm and detection probabilities for an ideal RF front-end ED detector, assuming flat fading Rayleigh channels and complex Gaussian transmitted signals. To the best of the authors' knowledge, this is the first time that such expressions are presented in the open technical literature, under these assumptions.
- Next, a signal model that describes the joint effects of all RF impairments is presented. This model is built upon an approximation of the joint effects of RF impairments by a complex Gaussian process [25] and is tractable to algebraic manipulations.

- Analytical closed-form expressions are provided for the evaluation of false alarm and detection probabilities of multi-channel EDs constrained by RF impairments, under Rayleigh fading. Based on this framework, the joint effects of RF impairments on spectrum sensing performance are investigated.
- Finally, we address an analytical study for the detection capabilities of cooperative spectrum sensing scenarios considering both cases of ideal ED detectors and multi-channel EDs constrained by RF impairments.

The remainder of the paper is organized as follows. The system and signal model for both ideal and hardware impaired RF front-ends are described in Section II. The analytical framework for evaluating the false alarm and detection probabilities, when both ideal sensing or RF imperfections are considered, are provided in Section III. Moreover, analytical closed-form expression for deriving the false alarm and detection probabilities, when a cooperative spectrum sensing with decision fusion system is considered, are provided in Section IV. Numerical and simulation results that illustrate the detrimental effects of RF impairments in spectrum sensing are presented in Section V. Finally, Section VI concludes the paper by summarizing our main findings.

Notations: Unless otherwise stated, $(x)^*$ stands for the complex conjugate of x , whereas $\Re\{x\}$ and $\Im\{x\}$ represent the real and imaginary part of x , respectively. The operators $E[\cdot]$ and $|\cdot|$ denote the statistical expectation and the absolute value, respectively. The sign of a real number x is returned by the operator $\text{sign}(x)$. The operator $\text{card}(\mathcal{A})$ returns the cardinality of the set \mathcal{A} . $U(x)$ and $\exp(x)$ denote the unit step function and the exponential function, respectively. The lower [37, Eq. (8.350/1)] and upper incomplete Gamma functions [37, Eq. (8.350/2)] are represented by $\gamma(\cdot, \cdot)$ and $\Gamma(\cdot, \cdot)$, respectively, while the Gamma function [37, Eq. (8.310)] is denoted by $\Gamma(\cdot)$. Moreover, $\Gamma(a, x, b, \beta) = \int_x^\infty t^{a-1} \exp(-t - bt^{-\beta}) dt$ is the extended incomplete Gamma function defined by [38, Eq. (6.2)]. Finally, $Q(x) = \frac{1}{\sqrt{2\pi}} \int_x^\infty \exp(-t^2/2) dt$ is the Gaussian Q-function.

II. SYSTEM AND SIGNAL MODEL

In this section, we briefly present the ideal signal model, which is referred to as ideal RF front-end in what follows. Build upon that, we demonstrate the practical signal model, where the RX is considered to suffer from RF imperfections, such as LNA nonlinearities, PHN and IQI. Note that it is assumed that K RF channels are down-converted to baseband using the wideband direct-conversion principle, which is referred to as multi-channel down-conversion [39].

A. Ideal RF front-end

The two hypothesis, namely absence/presence of primary user (PU), is denoted with parameter $\theta_k \in \{0, 1\}$. Suppose the n -th sample of the PU signal, $s(n)$, is conveyed over a flat-fading wireless channel, with channel gain, $h(n)$, and additive noise $w(n)$. The received wideband RF signal is passed through various RF front-end stages, including filtering, amplification, analog I/Q demodulation (down-conversion) to baseband and sampling. The wideband channel after sampling is assumed to have a bandwidth of W and contain K channels, each having bandwidth $W_{ch} = W_{sb} + W_{gb}$, where W_{sb} and W_{gb} are the signal band and total guard band bandwidth within this channel, respectively. Additionally, it is assumed that the sampling is performed with rate W . Note, that the rate of the signal is reduced by a factor of $L = W/W_{sb} \geq K$, where for simplicity we assume $L \in \mathbb{Z}$.

Under the ideal RF front-end assumption, after the selection filter, the n -th sample of the baseband equivalent received signal vector for the k^{th} channel ($k \in S \{-K/2, \dots, -1, 1, \dots, K/2\}$) is given by

$$r_k(n) = \Re\{r_k(n)\} + j\Im\{r_k(n)\} = \theta_k h_k(n) s_k(n) + w_k(n), \quad (1)$$

where h_k , s_k and w_k are zero-mean circular symmetric complex white Gaussian (CSCWG)

processes with variances σ_h^2 , σ_s^2 and σ_w^2 , respectively. Furthermore,

$$\Re \{r_k(n)\} = \theta_k \Re \{h_k(n)\} \Re \{s_k(n)\} - \theta_k \Im \{h_k(n)\} \Im \{s_k(n)\} + \Re \{w_k(n)\}, \quad (2)$$

$$\Im \{r_k(n)\} = \theta_k \Im \{h_k(n)\} \Re \{s_k(n)\} + \theta_k \Re \{h_k(n)\} \Im \{s_k(n)\} + \Im \{w_k(n)\}. \quad (3)$$

B. Non-ideal RF front-end

In the case of non-ideal RF front-end, the n -th sample of the impaired baseband equivalent received signal vector for the k^{th} channel is given by [14] and [17]

$$r_k(n) = \Re \{r_k(n)\} + j \Im \{r_k(n)\} = \xi_k(n) \theta_k h_k(n) s_k(n) + \eta_k(n) + w_k(n), \quad (4)$$

with

$$\Re \{r_k(n)\} = \theta_k \Re \{h_k(n) \xi_k\} \Re \{s_k(n)\} - \theta_k \Im \{h_k(n) \xi_k\} \Im \{s_k(n)\} + \Re \{\eta_k(n) + w_k(n)\}, \quad (5)$$

and

$$\Im \{r_k(n)\} = \theta_k \Im \{h_k(n) \xi_k\} \Re \{s_k(n)\} - \theta_k \Re \{h_k(n) \xi_k\} \Im \{s_k(n)\} + \Im \{\eta_k(n) + w_k(n)\}, \quad (6)$$

where ξ_k denotes the amplitude and phase rotation due to PHN caused by common phase error (CPE), LNA nonlinearities and IQI, and is given by

$$\xi_k = \gamma_0 K_1 \alpha, \quad (7)$$

while η_k denotes the distortion noise from impairments in the RX, and specifically due to PHN caused by inter carrier interference (ICI), IQI and non-linear distortion noise, and is given by

$$\eta_k(n) = K_1 (\gamma_0 e_k(n) + \psi_k(n)) + K_2 (\gamma_0^* (\alpha \theta_{-k} h_{-k}^*(n) s_{-k}^*(n) + e_{-k}^*(n))) + K_2 \psi_{-k}^*(n). \quad (8)$$

After denoting as $\Theta_k = \{\theta_{k-1}, \theta_{k+1}\}$ and $H_k = \{h_{k-1}, h_{k+1}\}$, this distortion noise term can be modeled as $\eta_k \sim \mathcal{CN}(0, \sigma_{\eta_k}^2)$, with

$$\sigma_{\eta_k}^2 = |\gamma_0|^2 (|K_1|^2 \sigma_{e,k}^2 + |K_2|^2 \sigma_{e,-k}^2) + |K_1|^2 \sigma_{\psi|H_k, \Theta_k}^2 + |K_2|^2 \sigma_{\psi|H_{-k}, \Theta_{-k}}^2 + |\gamma_0|^2 |K_2|^2 |\alpha|^2 \theta_{-k} |h_{-k}|^2 \sigma_s^2. \quad (9)$$

It should be noted that this model has been supported and validated by many theoretical investigations and measurements [18], [19], [25], [29], [40]–[43].

Next, we describe how the various parameters in (7), (8) and (9) stem from the imperfections associated with the RF front-end.

LNA Nonlinearities: The parameters α and e_k represent the nonlinearity parameters, which model the amplitude/phase distortion and the nonlinear distortion noise, respectively. According to Bussgang's theorem [44], e_k is a zero-mean Gaussian error term with variance $\sigma_{e_k}^2$. Considering an ideal clipping power amplifier (PA), the amplification factor α and the variance $\sigma_{e_k}^2$, are given by

$$\alpha = 1 - \exp(-\text{IBO}) + \sqrt{2\pi} \text{IBO} Q(2 \text{IBO}), \quad (10)$$

$$\sigma_{e_k}^2 = \sigma_s^2 (1 - \alpha^2 - \exp(-\text{IBO})), \quad (11)$$

where $\text{IBO} = A_o^2/\sigma_s^2$ denotes the input back-off factor and A_o is the PA's clipping level.

Furthermore, if a polynomial model is employed to describe the effects of nonlinearities, the amplification factor α and the variance σ_{e_k} , are given by

$$\alpha = \sum_{n=0}^{M-1} \beta_{n+1} 2^{-n/2} \sigma_s^2 \Gamma(1 + n/2), \quad (12)$$

$$\sigma_{e_k} = \sum_{n=2}^{2M} \gamma_n 2^{-n/2} \sigma_s^2 \Gamma(1 + n/2) - |a|^2 \sigma_s^2, \quad (13)$$

where

$$\gamma_n = \sum_{m=1}^{n-1} \hat{\beta}_m \hat{\beta}_{n-m}^*, \quad \text{and} \quad \hat{\beta}_m = \begin{cases} \beta_m, & 1 \leq m \leq M+1 \\ 0, & m > M+1 \end{cases} \quad (14)$$

I/Q Imbalance: The IQI coefficients K_1 and K_2 are given by

$$K_1 = \frac{1 + \epsilon e^{-j\theta}}{2} \quad \text{and} \quad K_2 = \frac{1 - \epsilon e^{j\theta}}{2}, \quad (15)$$

with ϵ and θ denote the amplitude and phase mismatch, respectively. It is noted that for perfect I/Q matching, this imbalance parameters become $\epsilon = 1$, $\theta = 0$; thus in this case $K_1 = 1$ and

$K_2 = 0$. The coefficients K_1 and K_2 are related through $K_1 = 1 - K_2^*$ and the image rejection ratio (IRR), which determines the amount of attenuation of the image frequency band, namely $\text{IRR} = |K_1/K_2|^2$. With practical analog front-end electronics, IRR is typically in the range of 20 – 40 dB [23], [39], [45].

Phase noise: The parameter, γ_0 , stands for CPE, which is equal for all channels, and ψ_k represents the ICI from all other neighboring channels due to spectral regrowth caused by PHN. Notice that, since the typical 3 dB bandwidth values for the oscillator process is in the order of few tens or hundreds of Hz, with rapidly fading spectrum after this point (approximately 10dB/decade), for channel bandwidth that is typical few tens or hundreds KHz, the only effective interference is due to leakage from successive neighbors only [16]. Consequently, the ICI term can be approximated as [16]

$$\psi_k(n) \approx \theta_{k-1} \gamma(n) h_{k-1}(n) s_{k-1}(n) + \theta_{k+1} \gamma(n) h_{k+1}(n) s_{k+1}(n), \quad (16)$$

with $\gamma(n) = \exp(j\phi(n))$ and $\phi(n)$ being a discrete Brownian error process, i.e., $\phi(n) = \sum_{m=1}^n \phi(m-1) + \epsilon(n)$, where $\epsilon(n)$ is a zero mean real Gaussian variable with variance $\sigma_\epsilon^2 = \frac{4\pi\beta}{W}$ and β being the 3 dB bandwidth of the local oscillator process.

The interference term ψ_k in (8) might have zero or non-zero contribution depending on the existence of PU signals in the successive neighboring channels. In general, this term is typically non-white and strictly speaking cannot be modeled by a Gaussian process. However, for practical 3 dB bandwidth of the oscillator process, the influence of the regarded impairments can all be modeled as a zero-mean Gaussian process with $\sigma_{\psi_k|\{H_k, \Theta_k\}}^2$ given by

$$\sigma_{\psi_k|\{H_k, \Theta_k\}}^2 = \theta_{k-1} A_{k-1} |h_{k-1}(n)|^2 \sigma_s^2 + \theta_{k+1} A_{k+1} |h_{k+1}(n)|^2 \sigma_s^2, \quad (17)$$

where

$$A_{k-1} = \frac{|I(f_{k-1} - f_k + f_{\text{cut-off}}) - I(f_{k-1} - f_k - f_{\text{cut-off}})|}{2\pi f_{\text{cut-off}}}, \quad (18)$$

$$A_{k+1} = \frac{|I(f_{k+1} - f_k + f_{\text{cut-off}}) - I(f_{k+1} - f_k - f_{\text{cut-off}})|}{2\pi f_{\text{cut-off}}}, \quad (19)$$

and f_k is the centered normalized frequency of the k^{th} channel, i.e., $f_k = \text{sign}(k) \frac{2|k|-1}{2K}$ and $f_{\text{cut-off}}$ is the normalized cut-off frequency of the k^{th} channel, which can be obtained by $f_{\text{cut-off}} = \frac{W_{sb}}{2W}$.

Furthermore,

$$\begin{aligned} I(f) &= (f_{\text{cut-off}} - f) \tan^{-1}(\delta \tan(\pi(f_{\text{cut-off}} - f))) + (f_{\text{cut-off}} + f) \tan^{-1}(\delta \tan(-\pi(f_{\text{cut-off}} + f))) \\ &\quad - \frac{1}{\delta} ((f_{\text{cut-off}} + f) \cot(\pi(f_{\text{cut-off}} + f)) - (f_{\text{cut-off}} - f) \cot(\pi(f_{\text{cut-off}} - f))) \\ &\quad + \frac{1}{\pi\delta} (\log(|\sin(\pi(f_{\text{cut-off}} + f))|) + \log(|\sin(\pi(f_{\text{cut-off}} - f))|)), \end{aligned} \quad (20)$$

with $\delta = \frac{\exp(-2\pi\beta/W)+1}{\exp(-2\pi\beta/W)-1}$. Due to Eqs. (18) and (19), it follows that $A_{k-1} = A_{k+1}$.

Joint effect of RF impairments: Here, we explain the joint impact of RF imperfections in the spectra of the down-converted received signal. Comparing Eq. (4) with Eq. (1), we observe that the RF imperfections result to not only amplitude/phase distortion, but also neighbor and mirror interference, as demonstrated intuitively in Fig. 1.

According to (7) and (9), LNA nonlinearities cause amplitude/phase distortion and an additive nonlinear distortion noise, whereas, based on (17), PHN causes interference to the received baseband signal at the k^{th} channel, due to the received baseband signals at the neighbor channels $k-1$ and $k+1$.

Moreover, based on (9), the joint effects of PHN and IQI, described by the terms $|K_1|^2 \sigma_{\psi|H_k, \Theta_k}^2$, $|K_2|^2 \sigma_{\psi|H_{-k}, \Theta_{-k}}^2$ and $|\gamma_0|^2 |K_2|^2 |\alpha|^2 \theta_{-k} |h_{-k}|^2 \sigma_s^2$, result to interference to the signal at the k^{th} ($k \in \{-\frac{K}{2} + 1, \dots, \frac{K}{2} + 1\}$) channel by the signals at the channels $-k-1$, $-k$, $-k+1$, $k-1$ and $k+1$. Note that if $k = -\frac{K}{2}$ or $k = \frac{K}{2}$, then PHN and IQI cause interference to the signal at the k^{th} channel due to the signals at the channels $-k$, $-k+1$ and $k-1$. Consequently, in this case, the terms that refer to the signals at the channels $-k-1$ and $k+1$ should be omitted.

Furthermore, the joint effects of LNA nonlinearities and IQI are described by the first term and the last terms in (9), i.e., $|K_1|^2 \sigma_{e,k}^2 + |K_2|^2 \sigma_{e,-k}^2$ and $|\gamma_0|^2 |K_2|^2 |\alpha|^2 \theta_{-k} |h_{-k}|^2 \sigma_s^2$, respectively, and result to additive distortion noises and mirror channel interference. Finally, the amplitude and phase distortion caused by the joint effects of all RF imperfections are modeled by the

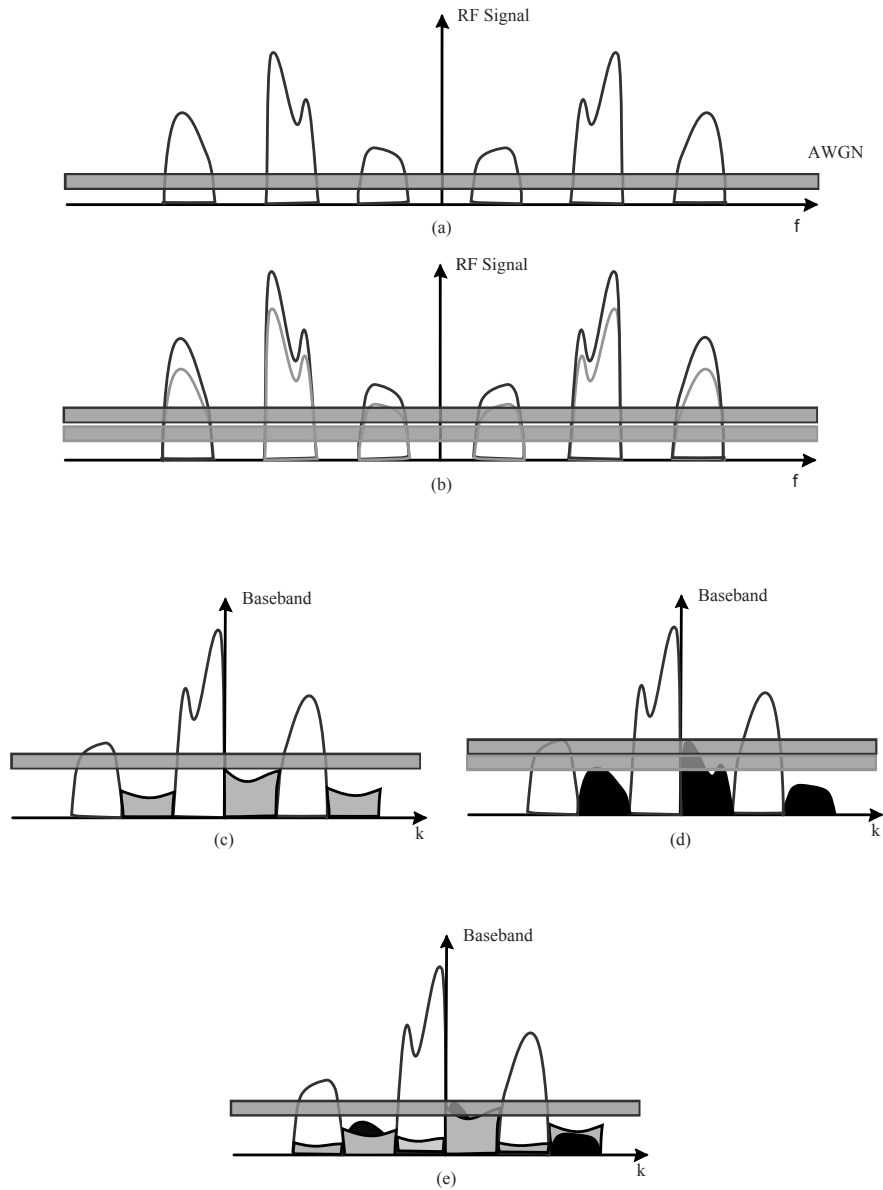


Fig. 1: Spectra of the received signal: (a) before LNA (passband RF signal), (b) after LNA (passband RF signal), (c) after down-conversion (baseband signal), when local oscillator's PHN is considered to be the only RF imperfection, (d) after down-conversion (baseband signal), when IQI is considered to be the only RF imperfection, (e) after down-conversion (baseband signal), the joint effect of LNA nonlinearities, PHN and IQI.

parameter ξ described in (7).

III. FALSE ALARM/DETECTION PROBABILITIES FOR CHANNEL DETECTION

In the classical ED, the energy of the received signals is used to determine whether a channel is idle or busy. Based on the signal model described in Section II, the ED calculates the test statistics for the k channel as

$$T_k = \frac{1}{N_s} \sum_{m=0}^{N_s-1} |r_k(n)|^2 = \frac{1}{N_s} \sum_{m=0}^{N_s-1} \Re \{r_k(n)\}^2 + \Im \{r_k(n)\}^2, \quad (21)$$

where N_s is the number of complex samples used for sensing. This test statistic is compared against a threshold $\gamma_{th}(k)$ to yield the sensing decision, i.e., the ED decides that the channel k is busy if $T_k > \gamma_{th}(k)$ or idle otherwise.

A. Ideal RF front-end

Based on the signal model presented in II-A and taking into consideration that

$$\sigma^2 = E[\Re \{r_k\}^2] = E[\Im \{r_k\}^2] = \theta_k (\Re \{h_k\}^2 + \Im \{h_k\}^2) \frac{\sigma_s^2}{2} + \frac{\sigma_w^2}{2}, \quad (22)$$

and $E[\Re \{r_k\} \Im \{r_k\}] = 0$ for a given channel realization h_k and channel occupation θ_k , the received energy follows chi-square distribution with $2N_s$ degrees of freedom and cumulative distribution function (CDF) given by

$$F_{T_k}(x | h_k, \theta_k) = \frac{\gamma(N_s, \frac{N_s x}{2\sigma^2})}{\Gamma(N_s)}. \quad (23)$$

The following theorem returns a closed-form expression for the CDF of the test statistics assuming that the channel is busy.

Theorem 1. *The CDF of the energy statistics assuming an ideal RF front end and a busy channel can be evaluated by*

$$F_{T_k}(x | \theta_k = 1) = 1 - \exp\left(-\frac{\sigma_w^2}{\sigma_h^2 \sigma_s^2}\right) \sum_{k=0}^{N_s-1} \frac{1}{k!} \left(\frac{N_s x}{\sigma_h^2 \sigma_s^2}\right)^k \Gamma\left(-k + 1, \frac{\sigma_w^2}{\sigma_h^2 \sigma_s^2}, \frac{N_s x}{\sigma_h^2 \sigma_s^2}, 1\right), \quad (24)$$

Proof: Since $h_k \sim \mathcal{CN}(0, \sigma_h^2)$, it follows that the parameter σ^2 follows exponential distribution with probability density function (PDF) given by

$$f_{\sigma^2}(x | \theta_k = 1) = \frac{2 \exp\left(\frac{\sigma_w^2}{\sigma_s^2 \sigma_h^2}\right)}{\sigma_s^2 \sigma_h^2} \exp\left(-\frac{2x}{\sigma_s^2 \sigma_h^2}\right), \quad (25)$$

with $x \in \left[\frac{\sigma_w^2}{2}, \infty\right)$. Hence, the unconditional CDF can be expressed as

$$F_{T_k}(x | \theta_k = 1) = \frac{1}{\Gamma(N_s)} \frac{2 \exp\left(\frac{\sigma_w^2}{\sigma_s^2 \sigma_h^2}\right)}{\sigma_s^2 \sigma_h^2} \int_{\frac{\sigma_w^2}{2}}^{\infty} \gamma\left(N_s, \frac{N_s x}{2y}\right) \exp\left(-\frac{2y}{\sigma_h^2 \sigma_s^2}\right) dy, \quad (26)$$

which is equivalent to

$$\begin{aligned} F_{T_k}(x | \theta_k = 1) &= \frac{1}{\Gamma(N_s)} \frac{2 \exp\left(\frac{\sigma_w^2}{\sigma_s^2 \sigma_h^2}\right)}{\sigma_s^2 \sigma_h^2} \int_{\frac{\sigma_w^2}{2}}^{\infty} \Gamma(N_s) \exp\left(-\frac{2y}{\sigma_h^2 \sigma_s^2}\right) dy \\ &\quad - \frac{1}{\Gamma(N_s)} \frac{2 \exp\left(\frac{\sigma_w^2}{\sigma_s^2 \sigma_h^2}\right)}{\sigma_s^2 \sigma_h^2} \int_{\frac{\sigma_w^2}{2}}^{\infty} \Gamma\left(N_s, \frac{N_s x}{2y}\right) \exp\left(-\frac{2y}{\sigma_h^2 \sigma_s^2}\right) dy, \end{aligned} \quad (27)$$

or

$$F_{T_k}(x | \theta_k = 1) = 1 - \frac{1}{\Gamma(N_s)} \frac{2 \exp\left(\frac{\sigma_w^2}{\sigma_s^2 \sigma_h^2}\right)}{\sigma_s^2 \sigma_h^2} \int_{\frac{\sigma_w^2}{2}}^{\infty} \Gamma\left(N_s, \frac{N_s x}{2y}\right) \exp\left(-\frac{2y}{\sigma_h^2 \sigma_s^2}\right) dy. \quad (28)$$

Since N_s is a positive integer, the upper incomplete Gamma function can be written as a finite sum [37, Eq. (8.352/2)], and hence (28) can be re-written as

$$F_{T_k}(x | \theta_k = 1) = 1 - \frac{2 \exp\left(\frac{\sigma_w^2}{\sigma_s^2 \sigma_h^2}\right)}{\sigma_s^2 \sigma_h^2} \sum_{k=0}^{N_s-1} \int_{\frac{\sigma_w^2}{2}}^{\infty} \frac{1}{k!} \left(\frac{N_s x}{2y}\right)^k \exp\left(-\frac{N_s x}{2y} - \frac{2y}{\sigma_h^2 \sigma_s^2}\right) dy. \quad (29)$$

After some algebraic manipulations and using [38, Eq. (6.2)], (29) can be written as in (24).

This concludes the proof. ■

Based on the above analysis, the false alarm probability for the ideal RX can be obtained by

$$\mathcal{P}_{fa}(\gamma) = P_r(T_k > \gamma | \theta_k = 0) = \frac{\Gamma\left(N_s, \frac{N_s \gamma}{\sigma_w^2}\right)}{\Gamma(N_s)}, \quad (30)$$

while the probability of detection can be calculated as

$$\mathcal{P}_d(\gamma) = P_r(T_k > \gamma | \theta_k = 1) = \exp\left(\frac{\sigma_w^2}{\sigma_h^2 \sigma_s^2}\right) \sum_{k=0}^{N_s-1} \frac{1}{k!} \left(\frac{N_s \gamma}{\sigma_h^2 \sigma_s^2}\right)^k \Gamma\left(-k + 1, \frac{\sigma_w^2}{\sigma_h^2 \sigma_s^2}, \frac{N_s \gamma}{\sigma_h^2 \sigma_s^2}, 1\right). \quad (31)$$

B. Non-Ideal RF Front-End

Based on the signal model presented in II-B, and assuming given channel realization and channel occupancy vectors $H = \{H_{-k}, h_{-k}, h_k, H_k\}$ and $\Theta = \{\Theta_{-k}, \theta_{-k}, \theta_k, \Theta_k\}$, respectively, it holds that

$$\sigma^2 = E[\Re\{r_k\}^2] = E[\Im\{r_k\}^2] = \theta_k (\Re\{h_k\}^2 + \Im\{h_k\}^2) (\Re\{\xi_k\}^2 + \Im\{\xi_k\}^2) \frac{\sigma_s^2}{2} + \frac{\sigma_w^2 + \sigma_{\eta_k}^2}{2}, \quad (32)$$

and $\Re\{r_k\}$, $\Im\{r_k\}$ are uncorrelated random variables, i.e., $E[\Re\{r_k\} \Im\{r_k\}] = 0$. Thus, the received energy, given by (21), follows chi-square distribution with $2N_s$ degrees of freedom and CDF given by

$$F_{T_k}(x | H, \Theta) = \frac{\gamma(N_s, \frac{N_s x}{2\sigma^2})}{\Gamma(N_s)}, \quad (33)$$

where σ^2 can be expressed, after taking into account (9), (17) and (32), as

$$\begin{aligned} \sigma^2 = & \theta_k \mathcal{A}_1 |h_k|^2 + \theta_{k-1} \mathcal{A}_2 |h_{k-1}|^2 + \theta_{k+1} \mathcal{A}_2 |h_{k+1}|^2 + \theta_{-k+1} \mathcal{A}_3 |h_{-k+1}|^2 \\ & + \theta_{-k-1} \mathcal{A}_3 |h_{-k-1}|^2 + \theta_{-k} \mathcal{A}_4 |h_{-k}|^2 + \mathcal{A}_5. \end{aligned} \quad (34)$$

In the above equation, $\mathcal{A}_1 = |\xi_k|^2 \frac{\sigma_s^2}{2}$, $\mathcal{A}_2 = |K_1|^2 A_{k-1} \frac{\sigma_s^2}{2}$, $\mathcal{A}_3 = |K_2|^2 A_{-k+1} \frac{\sigma_s^2}{2}$, $\mathcal{A}_4 = |\gamma_0|^2 |K_2|^2 |a|^2 \frac{\sigma_s^2}{2}$, and $\mathcal{A}_5 = \frac{\sigma_w^2}{2} + \frac{|\gamma_0|^2}{2} (|K_1|^2 \sigma_{e,k}^2 + |K_2|^2 \sigma_{e,-k}^2)$ model the amplitude distortion due to the joint effects of RF impairments, the interference from the $k-1$ and $k+1$ channels, the interference from the $-k-1$ and $-k+1$ channels due to PHN, the mirror interference due to IQI, and the distortion noise due to the joint effects of RF impairments, respectively.

The following theorems return analytical closed-form expressions for the CDF of the energy test statistics for a given channel occupancy vector, when at least one channel of $\{-k-1, -k, -k+1, k-1, k, k+1\}$ is busy and when all channels are idle.

Theorem 2. *The CDF of the energy statistics assuming an non-ideal RF front end and an arbitrary channel occupancy vector Θ that is different than the all idle vector, can be evaluated by (35), given at the top of the next page, where $w_{1,i}$ and $w_{2,i}$ are given by*

$$\begin{aligned}
F_{T_k}(x|\Theta) &= \sum_{i=2}^3 U(m_i - 2) w_{1,i} w_{2,i} \mathcal{A}_i \exp\left(-\frac{\mathcal{A}_5}{\mathcal{A}_i}\right) + \sum_{i=1}^4 U(m_i - 2) w_{1,i} \mathcal{A}_i (\mathcal{A}_5 + \mathcal{A}_i) \exp\left(-\frac{\mathcal{A}_5}{\mathcal{A}_i}\right) \\
&+ \sum_{i=1}^4 U(m_i - 1) (U(1 - m_i) - \mathcal{A}_5 U(m_i - 2)) w_{1,i} \mathcal{A}_i \exp\left(-\frac{\mathcal{A}_5}{\mathcal{A}_i}\right) \\
&- \sum_{i=2}^3 \sum_{k=0}^{N_s-1} U(m_i - 2) \frac{1}{k!} \frac{w_{1,i} w_{2,i}}{\mathcal{A}_i^{k-1}} \left(\frac{N_s x}{2}\right)^k \Gamma\left(-k + 1, \frac{\mathcal{A}_5}{\mathcal{A}_i}, \frac{N_s x}{2\mathcal{A}_i}, 1\right) \\
&- \sum_{i=1}^4 \sum_{k=0}^{N_s-1} U(m_i - 1) (U(1 - m_i) - \mathcal{A}_5 U(m_i - 2)) \frac{1}{k!} \frac{w_{1,i}}{\mathcal{A}_i^{k-1}} \left(\frac{N_s x}{2}\right)^k \Gamma\left(-k + 1, \frac{\mathcal{A}_5}{\mathcal{A}_i}, \frac{N_s x}{2\mathcal{A}_i}, 1\right) \\
&- \sum_{i=1}^4 \sum_{k=0}^{N_s-1} U(m_i - 2) \frac{1}{k!} \frac{w_{1,i}}{\mathcal{A}_i^{k-1}} \left(\frac{N_s x}{2}\right)^k \Gamma\left(-k + 2, \frac{\mathcal{A}_5}{\mathcal{A}_i}, \frac{N_s x}{2\mathcal{A}_i}, 1\right). \tag{35}
\end{aligned}$$

$$w_{1,i} = \frac{\exp\left(\frac{\mathcal{A}_5}{\mathcal{A}_i}\right)}{\Gamma(m_i) \left(\prod_{j=1}^4 \mathcal{A}_j^{m_j}\right)} \prod_{j=1, j \neq i}^4 \left(\frac{1}{\mathcal{A}_j} - \frac{1}{\mathcal{A}_i}\right)^{-m_j}, \tag{36}$$

and

$$w_{2,i} = \sum_{j=1, j \neq i} m_j \left(\frac{1}{\mathcal{A}_j} - \frac{1}{\mathcal{A}_i}\right)^{-1}, \tag{37}$$

respectively.

Proof: According to [46] and after some basic algebraic manipulations, its PDF can be written as

$$\begin{aligned}
f_{\sigma^2}(x|\Theta) &= \sum_{i=2}^3 U(m_i - 2) w_{1,i} w_{2,i} \exp\left(-\frac{x}{\mathcal{A}_i}\right) \\
&+ \sum_{i=1}^4 U(m_i - 1) (U(1 - m_i) - \mathcal{A}_5 U(m_i - 2)) w_{1,i} \exp\left(-\frac{x}{\mathcal{A}_i}\right) \\
&+ \sum_{i=1}^4 U(m_i - 1) U(m_i - 2) w_{1,i} x \exp\left(-\frac{x}{\mathcal{A}_i}\right), \tag{38}
\end{aligned}$$

where $x \in [\mathcal{A}_5, \infty)$, $m = [\theta_k, \theta_{k-1} + \theta_{k+1}, \theta_{-k+1} + \theta_{-k-1}, \theta_{-k}]$, $w_{1,i}$ and $w_{2,i}$ are defined by (36) and (37) respectively.

Based on the above, the CDF of the received energy, in case of non-ideal RF front-end, unconditioned with respect to Θ , can be expressed as

$$F_{T_k}(x|\Theta) = \sum_{i=2}^3 U(m_i - 2) w_{1,i} w_{2,i} \mathcal{I}_{1,i} + \sum_{i=1}^4 U(m_i - 1) (U(1 - m_i) - \mathcal{A}_5 U(m_i - 2)) w_{1,i} \mathcal{I}_{1,i} + \sum_{i=1}^4 U(m_i - 1) U(m_i - 2) w_{1,i} \mathcal{I}_{2,i}, \quad (39)$$

with

$$\mathcal{I}_{1,i} = \frac{1}{\Gamma(N_s)} \int_{\mathcal{A}_5}^{\infty} \exp\left(-\frac{y}{\mathcal{A}_i}\right) \gamma\left(N_s, \frac{N_s x}{2y}\right) dy, \quad (40)$$

$$\mathcal{I}_{2,i} = \frac{1}{\Gamma(N_s)} \int_{\mathcal{A}_5}^{\infty} y \exp\left(-\frac{y}{\mathcal{A}_i}\right) \gamma\left(N_s, \frac{N_s x}{2y}\right) dy. \quad (41)$$

Eqs. (40) and (41), after some basic algebraic manipulations, and using [37, Eq. (8.352/2)] and [38, Eq. (6.2)], can be written as

$$\mathcal{I}_{1,i} = \mathcal{A}_i \exp\left(-\frac{\mathcal{A}_5}{\mathcal{A}_i}\right) - \sum_{k=0}^{N_s-1} \frac{(N_s - 1)!}{k!} \left(\frac{N_s x}{2}\right)^k \frac{1}{\mathcal{A}_i^{k+1}} \frac{\Gamma\left(-k + 1, \frac{\mathcal{A}_5}{\mathcal{A}_i}, \frac{N_s x}{2\mathcal{A}_i}, 1\right)}{\Gamma(N_s)}, \quad (42)$$

and

$$\mathcal{I}_{2,i} = \mathcal{A}_i (\mathcal{A}_5 + \mathcal{A}_i) \exp\left(-\frac{\mathcal{A}_5}{\mathcal{A}_i}\right) - \sum_{k=0}^{N_s-1} \frac{(N_s - 1)!}{k!} \left(\frac{N_s x}{2}\right)^k \frac{1}{\mathcal{A}_i^{k+1}} \frac{\Gamma\left(-k + 2, \frac{\mathcal{A}_5}{\mathcal{A}_i}, \frac{N_s x}{2\mathcal{A}_i}, 1\right)}{\Gamma(N_s)}. \quad (43)$$

Hence, taking into consideration (42), (43) and since $U(m_i - 1)U(m_i - 2) = U(m_i - 2)$, Eq. (39) results to (35). This concludes the proof. \blacksquare

Theorem 3. *The CDF of the energy statistics assuming a non-ideal RF front-end and that the channel occupancy vector $\Theta = \tilde{\Theta}_{2,0} = [0, 0, 0, 0, 0, 0]$, can be obtained by*

$$F_{T_k}(x|\tilde{\Theta}_{2,0}) = \frac{\gamma\left(N_s, \frac{N_s x}{2\mathcal{A}_5}\right)}{\Gamma(N_s)}. \quad (44)$$

Proof: If the channel occupancy vector Θ is the all idle vector, i.e., $\Theta = \tilde{\Theta}_{2,0} = [0, 0, 0, 0, 0, 0]$, then, in accordance to (34), the signal variance can be expressed as $\sigma_{\tilde{\Theta}_{2,0}}^2 = \mathcal{A}_5$. According to (33), since $\sigma_{\tilde{\Theta}_{2,0}}^2$ is independent of H , the CDF of the energy statistics, assuming an non-ideal

RF front-end, when all the channels of $\{-k-1, -k, -k+1, k-1, k, k+1\}$ are idle, can be obtained by (44). This concludes the proof. \blacksquare

Based on the above analysis, the detection probability of the energy detector with RF impairments is

$$\mathcal{P}_D = \sum_{i=1}^{\text{card}(\tilde{\Theta}_1)} P_r(\tilde{\Theta}_1) \left(1 - F_{T_k}(\gamma^{\text{ni}} | \tilde{\Theta}_1)\right), \quad (45)$$

where $\tilde{\Theta}_1$ is the set defined as $\tilde{\Theta}_1 = [\theta_k = 1, \theta_{k-1}, \theta_{k+1}, \theta_{-k+1}, \theta_{-k-1}, \theta_{-k}]$. Similarly, the probability of false alarm is

$$\mathcal{P}_{FA} = \sum_{i=1}^{\text{card}(\tilde{\Theta}_{2,c})} P_r(\tilde{\Theta}_2) \left(1 - F_{T_k}(\gamma^{\text{ni}} | \tilde{\Theta}_{2,c})\right) + P_r(\tilde{\Theta}_{2,0}) \frac{\Gamma\left(N_s, \frac{N_s x}{2\mathcal{A}_5}\right)}{\Gamma(N_s)}, \quad (46)$$

where $\Pr(\Theta)$ denotes the probability of the given channel occupancy Θ , $\tilde{\Theta}_{2,c}$ is the set defined as $\tilde{\Theta}_{2,c} = \tilde{\Theta}_2 - \tilde{\Theta}_{2,0}$, and $\tilde{\Theta}_2$ is the set defined as $\tilde{\Theta}_2 = [\theta_k = 0, \theta_{k-1}, \theta_{k+1}, \theta_{-k+1}, \theta_{-k-1}, \theta_{-k}]$. Note that (46) applies even when the channel K or $-K$ is sensed. However, in this case $\tilde{\Theta}_1$ and $\tilde{\Theta}_2$ can be obtained by $\tilde{\Theta}_1 = [\theta_k = 1, \theta_{k-1}, \theta_{k+1} = 0, \theta_{-k+1}, \theta_{-k-1} = 0, \theta_{-k}]$ and $\tilde{\Theta}_2 = [\theta_k = 0, \theta_{k-1}, \theta_{k+1} = 0, \theta_{-k+1}, \theta_{-k-1} = 0, \theta_{-k}]$, respectively.

IV. COOPERATIVE SPECTRUM SENSING WITH DECISION FUSION

In this section, we consider a cooperative spectrum sensing scheme, in which each SU makes a binary decision on the channel occupancy, namely ‘0’ or ‘1’ for the absence or presence of PU activity, respectively, and the one-bit individual decisions are forwarded to a FC over a narrowband reporting channel. The sensing channels (the channels between the PU and the SUs) are considered identical and independent. Moreover, we assume that the decision device of the FC is implemented with the k_{SU} -out-of- n_{SU} rule, which implies that if there are k_{SU} or more SUs that individually decide that the channel is busy, the FC decides that the channel is occupied. Note that when $k_{\text{SU}} = 1$, $k_{\text{SU}} = n_{\text{SU}}$ or $k_{\text{SU}} = \lceil n/2 \rceil$, the k_{SU} -out-of- n_{SU} rule is simplified to the OR rule, AND rule and Majority rule, respectively.

A. Ideal RF Front-End

Here, we derive closed form expression for the false alarm and detection probabilities, assuming that the RF front-ends of the SUs are ideal, considering both scenarios of error free and imperfect reporting channels.

1) *Reporting Channels without Errors:* If the channel between the SUs and the FC is error free, the false alarm probability ($\mathcal{P}_{C,fa}$) and the detection probability ($\mathcal{P}_{C,d}$) are given by [8, Eq. (17)]

$$\mathcal{P}_{C,fa} = \sum_{i=k_{su}}^{n_{su}} \binom{n_{su}}{i} (\mathcal{P}_{fa})^i (1 - \mathcal{P}_{fa})^{n_{su}-i} \quad \text{and} \quad \mathcal{P}_{C,d} = \sum_{i=k_{su}}^{n_{su}} \binom{n_{su}}{i} (\mathcal{P}_d)^i (1 - \mathcal{P}_d)^{n_{su}-i}. \quad (47)$$

Taking into consideration (30) (31) and (24) and after some basic algebraic manipulations, Eqs. (47) can be expressed as

$$\mathcal{P}_{C,fa} = \sum_{i=k_{su}}^{n_{su}} \binom{n_{su}}{i} \left(\frac{\Gamma\left(N_s, \frac{N_s \gamma(k)}{\sigma_w^2}\right)}{\Gamma(N_s)} \right)^i \left(\frac{\gamma\left(N_s, \frac{N_s \gamma(k)}{\sigma_w^2}\right)}{\Gamma(N_s)} \right)^{n-i}, \quad (48)$$

$$\begin{aligned} \mathcal{P}_{C,d} &= \sum_{i=k_{su}}^{n_{su}} \binom{n_{su}}{i} \left(\exp\left(\frac{\sigma_w^2}{\sigma_h^2 \sigma_s^2}\right) \sum_{k=0}^{N_s-1} \frac{1}{k!} \left(\frac{N_s \gamma}{\sigma_h^2 \sigma_s^2}\right)^k \Gamma\left(-k+1, \frac{\sigma_w^2}{\sigma_h^2 \sigma_s^2}, \frac{N_s \gamma}{\sigma_h^2 \sigma_s^2}, 1\right)\right)^i \\ &\times \left(1 - \exp\left(\frac{\sigma_w^2}{\sigma_h^2 \sigma_s^2}\right) \sum_{k=0}^{N_s-1} \frac{1}{k!} \left(\frac{N_s \gamma}{\sigma_h^2 \sigma_s^2}\right)^k \Gamma\left(-k+1, \frac{\sigma_w^2}{\sigma_h^2 \sigma_s^2}, \frac{N_s \gamma}{\sigma_h^2 \sigma_s^2}, 1\right)\right)^{n_{su}-i}. \quad (49) \end{aligned}$$

2) *Reporting Channels with Errors:* If the reporting channel is imperfect, error occur on the detection of the transmitted, by the SU, bits. In this case, the false alarm and the detection probabilities can be derived by [8, Eq. (18)]

$$\mathcal{P}_{C,\mathcal{X}} = \sum_{i=k_{su}}^{n_{su}} \binom{n_{su}}{i} (\mathcal{P}_{\mathcal{X},e})^i (1 - \mathcal{P}_{\mathcal{X},e})^{n_{su}-i}, \quad (50)$$

where $\mathcal{P}_{\mathcal{X},e} = \mathcal{P}_{\mathcal{X}}(1 - P_e) + (1 - \mathcal{P}_{\mathcal{X}})P_e$, is the equivalent false alarm ($\mathcal{X} = fa$) or detection ($\mathcal{X} = d$) probability and P_e is the cross-over probability of the reporting channel, which is

equal to the bit error rate (BER) of the channel. Considering binary phase shift keying (BPSK), ideal RF front-end in the FC and Rayleigh fading, the BER can be expressed as

$$P_e = \frac{1}{2} \left(1 - \sqrt{\frac{\gamma_r}{1 + \gamma_r}} \right), \quad (51)$$

with γ_r be the signal to noise ratio (SNR) of the link between the SUs and the FC.

B. Non-Ideal RF Front-End

In this subsection, we consider that the RXs front-end of the SUs suffer from different level RF imperfections.

1) *Reporting Channels without Errors:* In this section, we assume that the reporting channel is error free and that the SU j sends $d_{j,k} = 0$ or $d_{j,k} = 1$ to the FC to report absence or presence of PU activity at the channel k .

If the sensing channel k is idle ($\theta_k = 0$), then the probability that the j^{th} SU reports that the channel is busy ($d_{j,k} = 1$), can be expressed as $\mathcal{P}_{fa,j}$, while the probability that the j^{th} SU reports that the channel is idle ($d_{j,k} = 0$), is given by $(1 - \mathcal{P}_{fa,j})$. Therefore, since each SU decides individually whether there is PU activity in the channel k , the probability that the n SUs report a given decision set $\mathcal{D} = [d_{1,k}, d_{2,k}, \dots, d_{n_{\text{su}},k}]$, if $\theta_k = 0$, can be written as

$$\mathcal{P}_{fa}(\mathcal{D}) = \prod_{j=1}^{n_{\text{su}}} (U(-d_{j,k})(1 - \mathcal{P}_{fa,j}) + U(d_{j,k} - 1)\mathcal{P}_{fa,j}). \quad (52)$$

Furthermore, based on the k_{su} -out-of- n_{su} rule, the FC decides that the k^{th} channel is busy, if the k_{su} out of the n_{su} SUs reports “1”. Consequently, for a given decision set, the false alarm probability at the FC can be evaluated by

$$\mathcal{P}_{C,FA|\mathcal{D}} = U \left(\sum_{l=1}^{n_{\text{su}}} d_{l,k} - k_{\text{su}} \right) \prod_{j=1}^{n_{\text{su}}} (U(-d_{j,k})(1 - \mathcal{P}_{fa,j}) + U(d_{j,k} - 1)\mathcal{P}_{fa,j}). \quad (53)$$

Hence, for any possible \mathcal{D} , the false alarm at the FC, using k_{su} -out-of- n_{su} rule, can be obtained by

$$\mathcal{P}_{C,FA} = \sum_{i=1}^{\text{card}(\mathcal{D})} U \left(\sum_{l=1}^{n_{\text{su}}} d_{l,k} - k_{\text{su}} \right) \prod_{j=1}^{n_{\text{su}}} (U(-d_{j,k})(1 - \mathcal{P}_{fa,j}) + U(d_{j,k} - 1)\mathcal{P}_{fa,j}). \quad (54)$$

Similarly, the detection probability at the FC, using k_{su} -out-of- n_{su} rule, can be expressed as

$$\mathcal{P}_{C,D} = \sum_{i=1}^{\text{card}(\mathcal{D})} U \left(\sum_{l=1}^{n_{\text{su}}} d_{l,k} - k_{\text{su}} \right) \prod_{j=1}^{n_{\text{su}}} (U(-d_{j,k})(1 - \mathcal{P}_{d,j}) + U(d_{j,k} - 1)\mathcal{P}_{d,j}). \quad (55)$$

Note that if the FC uses the OR rule, Eqs. (54) and (55) can be simplified to

$$\mathcal{P}_{\text{OR},FA} = 1 - \prod_{i=1}^{n_{\text{su}}} (1 - \mathcal{P}_{fa,i}), \quad \text{and} \quad \mathcal{P}_{\text{OR},D} = 1 - \prod_{i=1}^{n_{\text{su}}} (1 - \mathcal{P}_{d,i}), \quad (56)$$

respectively, while if the FC uses the AND rule, Eqs. (54) and (55) can be simplified to

$$\mathcal{P}_{\text{AND},FA} = \prod_{i=1}^{n_{\text{su}}} \mathcal{P}_{fa,i}, \quad \text{and} \quad \mathcal{P}_{\text{AND},D} = \prod_{i=1}^{n_{\text{su}}} \mathcal{P}_{d,i}, \quad (57)$$

respectively.

In the special case where all the SUs suffer from the same level of RF impairments, the false alarm probability ($\mathcal{P}_{C,fa}$) and the detection probability ($\mathcal{P}_{C,d}$) are given by

$$\mathcal{P}_{C,FA} = \sum_{i=k_{\text{su}}}^{n_{\text{su}}} \binom{n_{\text{su}}}{i} (\mathcal{P}_{FA})^i (1 - \mathcal{P}_{FA})^{n_{\text{su}}-i}, \quad \text{and} \quad \mathcal{P}_{C,D} = \sum_{i=k_{\text{su}}}^{n_{\text{su}}} \binom{n_{\text{su}}}{i} (\mathcal{P}_D)^i (1 - \mathcal{P}_D)^{n_{\text{su}}-i}, \quad (58)$$

where \mathcal{P}_{FA} and \mathcal{P}_D are given by (46) and (45), respectively.

2) *Reporting Channels with Errors:* Next, we consider an imperfect reporting channel. In this scenario, the false alarm and the detection probabilities can be derived by

$$\mathcal{P}_{C,\mathcal{X}} = \sum_{i=1}^{\text{card}(\mathcal{D})} U \left(\sum_{l=1}^{n_{\text{su}}} d_{l,k} - k_{\text{su}} \right) \prod_{j=1}^{n_{\text{su}}} (U(-d_{j,k})(1 - \mathcal{P}_{\mathcal{X},e,j}) + U(d_{j,k} - 1)\mathcal{P}_{\mathcal{X},e,j}), \quad (59)$$

where $\mathcal{P}_{\mathcal{X},e,j}$ can be derived by

$$\mathcal{P}_{\mathcal{X},e,j} = \mathcal{P}_{\mathcal{X},j} (1 - P_{e,j}) + (1 - \mathcal{P}_{\mathcal{X},j}) P_{e,j}, \quad (60)$$

with $\mathcal{P}_{\mathcal{X},j}$ denoting the equivalent false alarm ($\mathcal{X} = FA$) or detection ($\mathcal{X} = D$) probability of the j^{th} SU and $P_{e,j}$ being the cross-over probability of the reporting channel connecting the j^{th} SU with the FC. Notice that since $\mathcal{P}_{\mathcal{X},j} \in [0, 1]$, based on (60) $\mathcal{P}_{\mathcal{X},e,j}$ is bound by $P_{e,j}$ and $1 - P_{e,j}$.

In the special case where all the SUs suffer from the same level of RF impairments, Eq. (59) can be expressed as [8, Eq. (18)]

$$\mathcal{P}_{C,\mathcal{X}} = \sum_{i=k_{\text{su}}}^{n_{\text{su}}} \binom{n_{\text{su}}}{i} (\mathcal{P}_{\mathcal{X},e})^i (1 - \mathcal{P}_{\mathcal{X},e})^{n_{\text{su}}-i}. \quad (61)$$

V. NUMERICAL AND SIMULATION RESULTS

In this section, we investigate the effects of RF impairments on the spectrum sensing performance of EDs by illustrating analytical and Monte-Carlo simulation results for different RF imperfection levels. In particular, we consider the following insightful scenario. It is assumed that there are $K = 8$ channels and the second channel is sensed (i.e., $k = 2$). The signal and the total guard band bandwidths are assumed to be $W_{sb} = 1$ MHz and $W_{gb} = 125$ KHz, respectively, while the sampling rate is chosen to be equal to the bandwidth of wireless signal as $W = 9$ MHz. Moreover, the channel occupancy process is assumed to be Bernoulli distributed with probability, $q = 1/2$, and independent across channels, while the signal variance is equal for all channels. The number of samples is set to 5 ($N_s = 5$), while it is assumed that $\sigma_h^2 = \sigma_w^2 = 1$. In addition, for simplicity and without loss of generality, we consider an ideal clipping PA. In the following figures, the numerical results are shown with continuous lines, while markers are employed to illustrate the simulation results. Moreover, the performance of a classical ED with ideal RF front-end is used as a benchmark.

Figs. 2 and 3 demonstrate the impact of LNA non-linearities on the performance of the classical ED, assuming different SNR values. Specifically, in Fig. 2, false alarm probabilities are plotted against threshold for different SNR and IBO values, considering $\beta = 100$ Hz, IRR = 25 dB and phase imbalance equal to $\phi = 3^\circ$. It becomes evident from this figure that the analytical results are identical with simulation results; thus, verifying the presented analytical framework. Additionally, it is observed that for a given IBO value, as SNR increases, the interference for the neighbor and mirror channels increases; hence, the false alarm probability increases. On

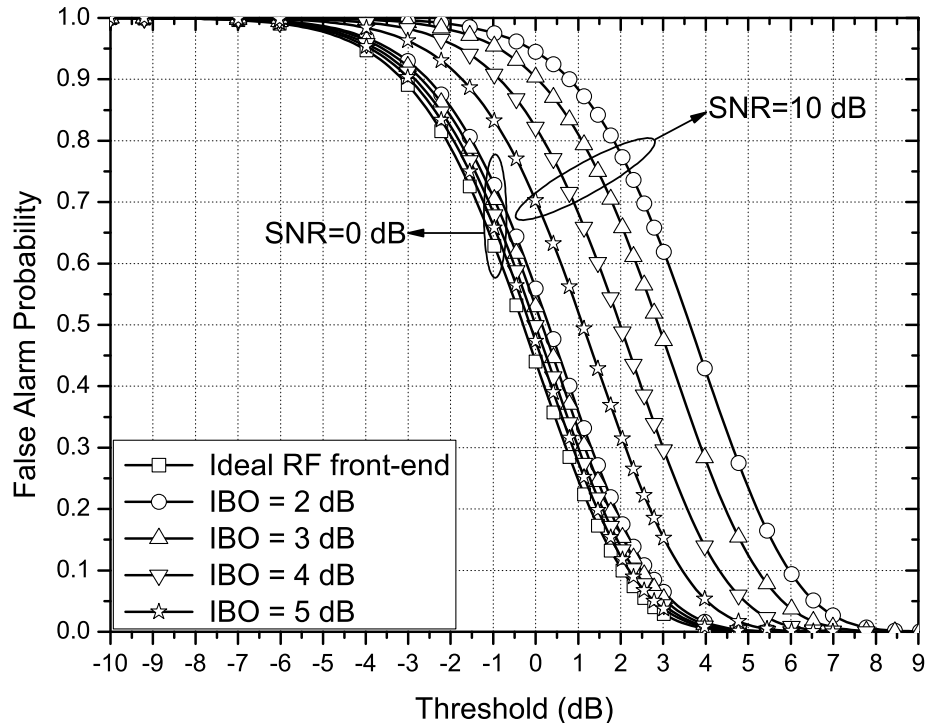


Fig. 2: False alarm probability vs Threshold for different values of IBO and occupied channel SNR values, when IRR and β are considered to be equal to 25dB and 100Hz, respectively.

the contrary as IBO increases, for a given SNR value, the effects of LNA non-linearities are constrained, and therefore the false alarm probability decreases.

In Fig. 3, receiver operation curves (ROCs) are plotted for different SNR and IBO values, considering the $\beta = 100$ Hz, IRR = 25 dB and $\phi = 3^\circ$. We observe that for low SNR values, LNA non-linearities do not affect the ED performance. However, as SNR increases, the distortion noise caused due to the imperfection of the amplifier increases; as a result, LNA non-linearities become to have more adverse effects on the spectrum capabilities of the classical ED, significantly reducing its performance for low IBO values. Furthermore, as IBO increases, the effects of LNA non-linearities become constrained and therefore the performance of the non-ideal ED tends to the performance of the ideal ED.

Fig.4 illustrates the impact of PHN on the performance of the classical ED, assuming various SNR values, when IRR = 25 dB, $\phi = 3^\circ$ and IBO = 6 dB. We observe that for practical levels

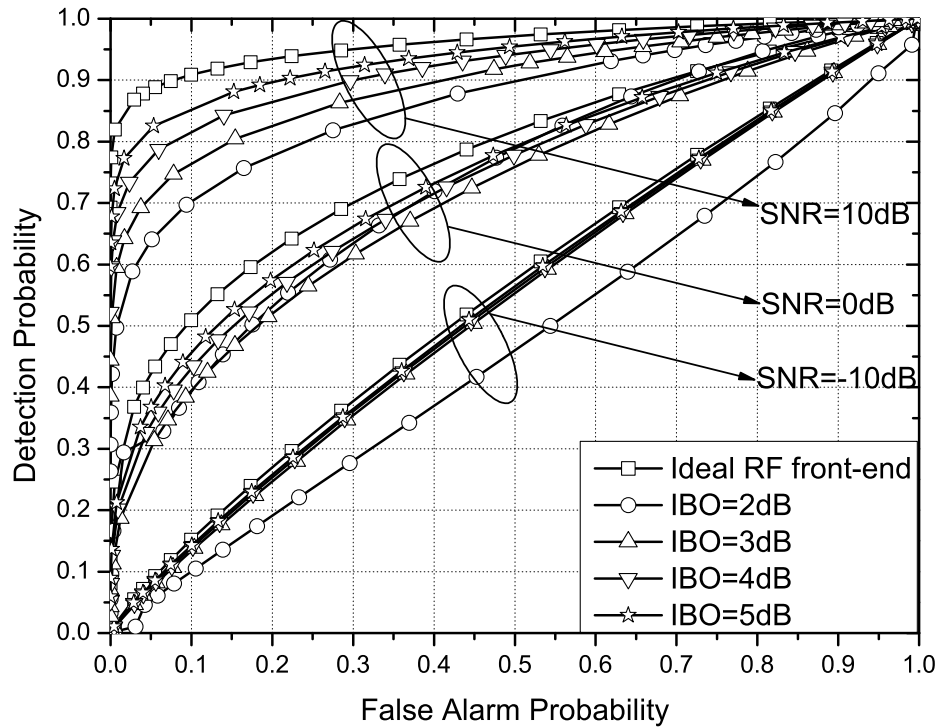


Fig. 3: ROC for different values of IBO and occupied channel SNR values, when IRR and β are considered to be equal to 25dB and 100Hz, respectively.

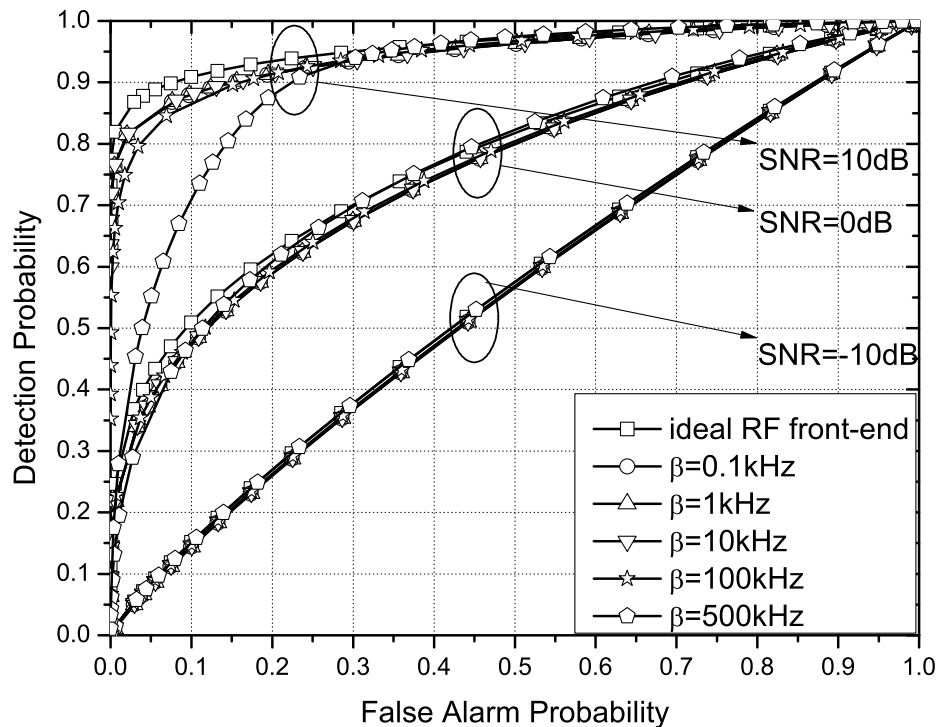


Fig. 4: ROCs for different values of β and occupied channel SNR values, when IBO and IRR are considered to be equal to 6dB and 25dB, respectively.

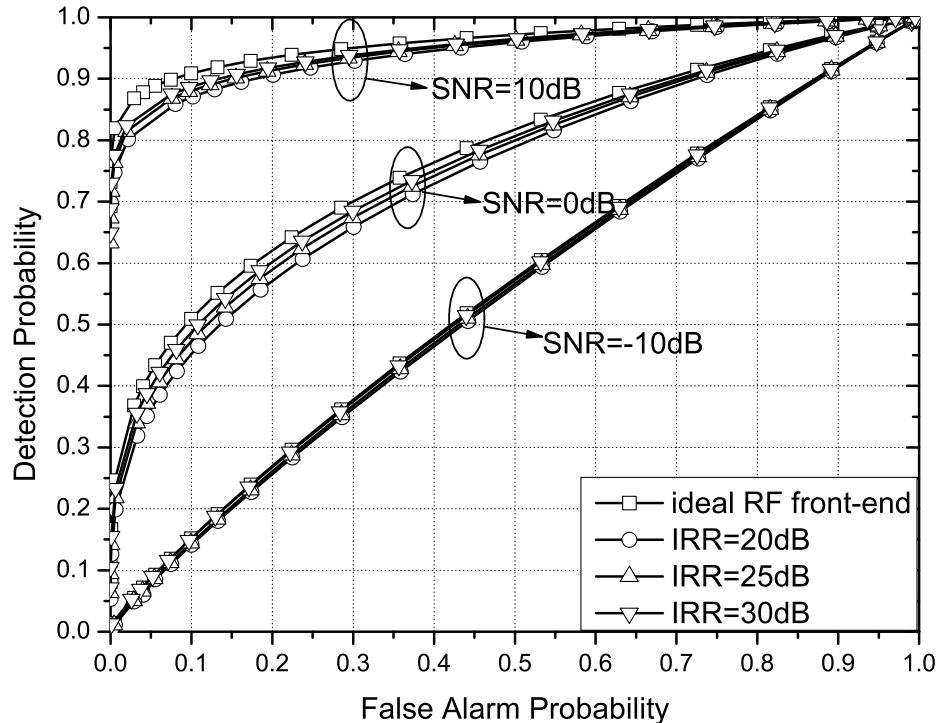


Fig. 5: ROCs for different values of IRR and occupied channel SNR values, when IBO and β are considered to be equal to 6dB and 100Hz, respectively.

of IQI and PHN, the signal leakage from channels $-k + 1$ and $-k - 1$ to channel $-k$ due to PHN is small, therefore the signal leakage to channel k from the channel $-k - 1$ and $-k + 1$ due to the joint effect of PHN and IQI is in the range of $[-70 \text{ dB}, -50 \text{ dB}]$. Consequently, in the low SNR regime the leakage from the channels $-k - 1$ and $-k + 1$ do not affect the spectrum sensing capabilities. Hence, it becomes evident that at low SNR values, PHN do not affect the spectrum sensing capability of the classical ED compared with the ideal RF front-end ED. On the other hand, as SNR increases, PHN has more detrimental effects on the spectrum sensing capabilities of the classical ED, significantly reducing the ED performance for high β values.

The effects of IQI on the spectrum sensing performance of ED are presented at Fig. 5. In particular, in this figure, ROCs are plotted assuming various SNRs, when the $IBO = 6 \text{ dB}$ and $\beta = 100 \text{ Hz}$. Again, the analytical results coincide with simulation results, verifying the derived expressions. Moreover, at low SNRs, it is observed that there is no significant performance

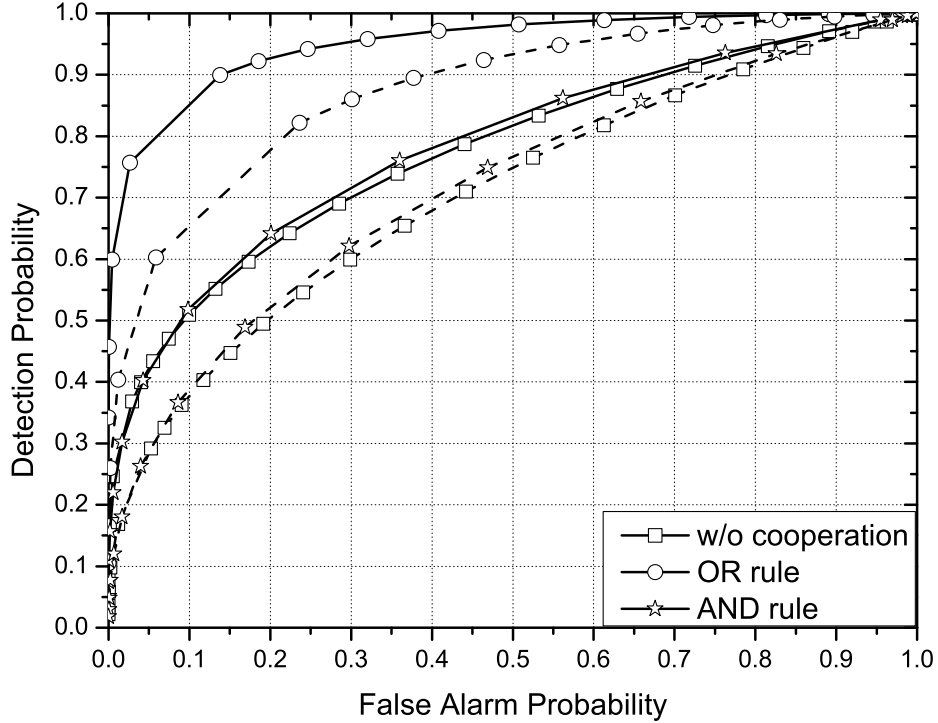


Fig. 6: ROCs for ideal (continuous line) and non-ideal (dashed lines) RF front-end , when the CR network is equipped with 5 SUs, $\text{SNR} = 0$ dB, the reporting channel is considered error free, and $\text{IBO} = 3$ dB, $\text{IRR} = 20$ dB, and $\beta = 100$ Hz, for all the SUs.

degradation due to IQI. Nonetheless, as SNR increases, the interference of the mirror channels increases and as a result this RF imperfection notably affects the spectrum sensing performance. Additionally, for a given SNR, we observe that as IRR increases, the signal leakage of the mirror channels, due to IQI, decreases; hence, the performance of the non-ideal ED tends to become identical to the one of the ideal ED. Finally, when compared with the spectrum sensing performance affected by LNA nonlinearities, as depicted in Fig. 3, it becomes apparent that the impact of LNA nonlinearity to the spectrum sensing performance is more detrimental than the impact of IQI.

The effects of RF impairments in cooperative sensing, when the reporting channel is considered error free, is illustrated in Fig. 6. In this figure, ROCs for ideal (continuous lines) and non-ideal (dashed lines) RF front-end SUs are presented, considering a CR network composed of $n_{\text{SU}} = 5$

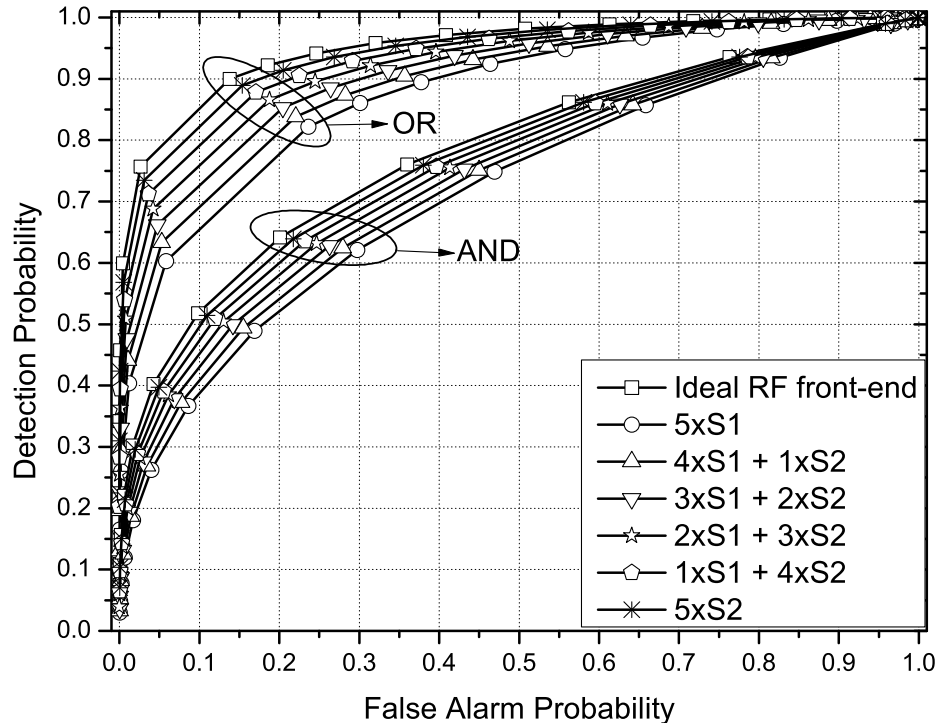


Fig. 7: ROCs for ideal and non-ideal RF front-end, when the CR network is equipped with 5 SUs under different levels of RF imperfections, $\text{SNR} = 0$ dB, the reporting channel is considered error free and the FC uses AND or OR rule. S_1 and S_2 stands for SUs with $\text{IBO} = 3$ dB and $\text{IRR} = 20$ dB, and $\text{IBO} = 6$ dB and $\text{IRR} = 300$ dB, respectively.

SUs, and a FC, which uses the OR or AND rule to decide whether the sensing channel is idle or busy. The EDs of the SUs are assumed identical with $\text{IBO} = 3$ dB, $\text{IRR} = 20$ dB, and 100 Hz 3 dB bandwidth. Again it is shown that the analytical results are identical with simulation results; thus, verifying the presented analytical framework. When a given decision rule is applied, it becomes evident from the figure that the RF imperfections cause severe degradation of the sensing capabilities of the CR network. For instance, if the OR rule is employed and false alarm probability is equal to 14%, the RF impairments results to about 31% degradation compared with the ideal RF front-end scenario. This result indicates that it is important to take into consideration the hardware constraints of the low-cost spectrum sensing SUs.

In Fig. 7, ROCs are illustrated for a CR network composed of $n = 5$ SUs, which suffer from

different levels of RF imperfections, and a FC that employs the AND or the OR rule to decide whether the sensing channel is idle or busy. In this scenario, we consider two types of SUs, namely S_1 and S_2 . The RF front-end specifications of S_1 are IBO = 3 dB, IRR = 20 dB and $\beta = 100$ Hz, whereas the specifications of S_2 are IBO = 6 dB, IRR = 30 dB and $\beta = 100$ Hz. In other words, the CR network, in this scenario, includes both SUs of almost the worst (S_1) and almost optimal (S_2) quality. As benchmarks, the ROCs of a CR network equipped with classical ED sensor nodes in which the RF front-end is considered to be ideal, and CR networks that uses only S_1 or only S_2 sensor nodes are presented. In this figure, we observe the detrimental effects of the RF imperfections of the ED sensor nodes to the sensing capabilities of the CR network. Furthermore, it is demonstrated that as the numbers of S_1 and S_2 SUs are decreasing and increasing respectively, the energy detection performance of the FC tends to become identical to the case when all the SUs are considered to be ideal. This was expected since S_2 SUs have higher quality RF front-end characteristics than the other set of SUs.

VI. CONCLUSIONS

We studied the performance of multi-channel spectrum sensing, when the RF front-end is impaired by hardware imperfections. In particular, assuming Rayleigh fading, we provided the analytical framework for evaluating the detection and false alarm probabilities of energy detectors when LNA nonlinearities, IQI and PHN are taken into account. Next, we extended our study to the case of a CR network, in which the SUs suffer from different levels of RF impairments, taking into consideration both scenarios of error free and imperfect reporting channels. Our results illustrated the degrading effects of RF imperfections on the ED spectrum sensing performance, which bring significant losses in the utilization of the spectrum. Among others, LNA nonlinearities were shown to have the most detrimental effect on the spectrum sensing performance. Furthermore, we observed that in cooperative spectrum sensing, the sensing capabilities of the CR system are significantly influenced by the different levels of RF imperfections of the SUs.

Therefore, hardware constraints should be seriously taken into consideration when designing direct conversion CR RXs.

APPENDIX

APPROXIMATION FOR EXTENDED INCOMPLETE GAMMA FUNCTION CALCULATION

Theorem 4. *The extended incomplete Gamma function can be approximated as*

$$\Gamma(a, x, b, 1) \approx \sum_{n=0}^N \frac{(-b)^n}{n!} \Gamma(a - n, x), \quad (62)$$

with an approximation error upper-bounded by

$$\epsilon(a, x, b, N) = \exp(b) \Gamma(a - N - 1, x) \frac{\gamma(N + 1, b)}{\Gamma(N + 1)}. \quad (63)$$

Proof: The extended incomplete Gamma function can be expanded in terms of the incomplete Gamma function as [38, Eq. (6.54)]

$$\Gamma(a, x, b, 1) = \sum_{n=0}^{\infty} \frac{(-b)^n}{n!} \Gamma(a - n, x). \quad (64)$$

By denoting $f(a, x, b, n) = \frac{b^n}{n!} \Gamma(a - n, x)$, the extended incomplete gamma function can be rewritten as $\Gamma(a, x, b, 1) = \sum_{n=0}^{\infty} (-1)^n f(a, x, b, n)$. Moreover, according to [38, Eq. (3.84)], the auxiliary function $f(a, x, b, n)$ is equivalent to $f(a, x, b, n) = \frac{b^n}{n!} \frac{E_{n-a+1}(x)}{x^{n-a}}$, where $E_n(x)$ is the exponential integral function defined in [47, Eq. (5.1.4)]. Taking into consideration the property [47, Eq. (5.1.17)], it follows that for given parameters $a, x > 0$ and n ,

$$\Gamma(a - n, x) \geq \Gamma(a - n - 1, x), \quad (65)$$

and, hence, for a given $b > 0$,

$$\lim_{n \rightarrow \infty} f(a, x, b, n) = 0. \quad (66)$$

Thus, the extended incomplete gamma function can be approximated by (62) where the approximation error is given by

$$e(a, x, b, N) = \sum_{n=N+1}^{\infty} (-1)^n f(a, x, b, n), \quad (67)$$

which can be upper-bounded, according to (65) and (66), as

$$e(a, x, b, N) \leq \sum_{n=N+1}^{\infty} f(a, x, b, n) \leq \Gamma(a - N - 1, x) \sum_{n=N+1}^{\infty} \frac{b^n}{n!}. \quad (68)$$

Hence, using [37, Eq. (1.211/1)] and [37, Eq. (8.352/2)], the upper bound on the approximation error given by (63) is derived. ■

REFERENCES

- [1] FCC, “Spectrum policy task force report,” November 2002.
- [2] E. H. Gismalla and E. Alsusa, “On the performance of energy detection using Bartlett’s estimate for spectrum sensing in cognitive radio systems,” *IEEE Trans. Signal Process.*, vol. 60, no. 7, pp. 3394–3404, Jul. 2012.
- [3] T. Yucek and H. Arslan, “A survey of spectrum sensing algorithms for cognitive radio applications,” *IEEE Communications Surveys & Tutorials*, vol. 11, no. 1, pp. 116–130, Mar. 2009.
- [4] O. Altrad, S. Muhaidat, A. Al-Dweik, A. Shami, and P. D. Yoo, “Opportunistic spectrum access in cognitive radio networks under imperfect spectrum sensing,” *IEEE Trans. Veh. Technol.*, vol. 63, no. 2, pp. 920–925, Feb. 2014.
- [5] M. Seyf, S. Muhaidat, and J. Liang, “Relay selection in cognitive radio networks with interference constraints,” *IET Communications*, vol. 7, no. 10, pp. 922–930, Jul. 2013.
- [6] L. Fan, X. Lei, T. Q. Duong, R. Q. Hu, and M. ElKashlan, “Multiuser cognitive relay networks: Joint impact of direct and relay communications,” *IEEE Trans. Wireless Commun.*, vol. 13, no. 9, pp. 5043–5055, Sep. 2014.
- [7] W. Xu, W. Xiang, M. ElKashlan, and H. Mehrpouyan, “Spectrum sensing of OFDM signals in the presence of carrier frequency offset,” *IEEE Trans. Veh. Technol.*, no. 99, pp. 1–1, Sep. 2015.
- [8] S. Atapattu, C. Tellambura, and H. Jiang, “Energy detection based cooperative spectrum sensing in cognitive radio networks,” *IEEE Trans. Commun.*, vol. 10, no. 4, pp. 1232–1241, Apr. 2011.
- [9] M. Z. Shakir, A. Rao, and M.-S. Alouini, “Generalized mean detector for collaborative spectrum sensing,” *IEEE Trans. Commun.*, vol. 61, no. 4, pp. 1242–1253, Apr. 2013.
- [10] D. Hamza, S. Aissa, and G. Aniba, “Equal gain combining for cooperative spectrum sensing in cognitive radio networks,” *IEEE Trans. Wireless Commun.*, vol. 13, no. 8, pp. 4334–4345, Aug. 2014.
- [11] W. Zhang, R. Mallik, and K. Letaief, “Optimization of cooperative spectrum sensing with energy detection in cognitive radio networks,” *IEEE Trans. Wireless Commun.*, vol. 8, no. 12, pp. 5761–5766, Dec. 2009.
- [12] A. Kortun, T. Ratnarajah, M. Sellathurai, C. Zhong, and C. Papadias, “On the performance of eigenvalue-based cooperative spectrum sensing for cognitive radio,” *IEEE J. Sel. Topics Signal Process.*, vol. 5, no. 1, pp. 49–55, Feb. 2011.
- [13] A. Al Hammadi, O. Alhussein, P. Sofotasios, S. Muhaidat, M. Al-Qutayri, S. Al-Araji, G. Karagiannidis, and J. Liang, “Unified analysis of cooperative spectrum sensing over composite and generalized fading channels,” *IEEE Trans. Veh. Technol.*, no. 99, pp. 1–1, Oct. 2015.

- [14] A. Gokceoglu, S. Dikmese, M. Valkama, and M. Renfors, "Energy detection under IQ imbalance with single- and multi-channel direct-conversion receiver: Analysis and mitigation," *IEEE J. Sel. Areas Commun.*, vol. 32, no. 3, pp. 411–424, Mar. 2014.
- [15] B. Razavi, "Cognitive radio design challenges and techniques," *IEEE J. Solid-State Circuits*, vol. 45, no. 8, pp. 1542–1553, Aug. 2010.
- [16] A. Gokceoglu, Y. Zou, M. Valkama, and P. C. Sofotasios, "Multi-channel energy detection under phase noise: analysis and mitigation," *Mobile Networks and Applications*, vol. 19, no. 4, pp. 473–486, May 2014.
- [17] T. Schenk, *RF Imperfections in High-Rate Wireless Systems*. The Netherlands: Springer, 2008.
- [18] M. Wenk, *MIMO-OFDM Testbed: Challenges, Implementations, and Measurement Results*, ser. Series in microelectronics. ETH, 2010.
- [19] C. Studer, M. Wenk, and A. Burg, "System-level implications of residual transmit-RF impairments in MIMO systems," in *Proceedings of the 5th European Conference on Antennas and Propagation (EUCAP)*, Apr. 2011, pp. 2686–2689.
- [20] E. Bjornson, M. Matthaiou, and M. Debbah, "A new look at dual-hop relaying: Performance limits with hardware impairments," *IEEE Trans. Commun.*, vol. 61, no. 11, pp. 4512–4525, Nov. 2013.
- [21] J. Verlant-Chenet, J. Renard, J.-M. Dricot, P. D. Doncker, and F. Horlin, "Sensitivity of spectrum sensing techniques to RF impairments," in *IEEE 71st Vehicular Technology Conference (VTC 2010-Spring)*, May 2010, pp. 1–5.
- [22] A. Zahedi-Ghasabeh, A. Tarighat, and B. Daneshrad, "Cyclo-stationary sensing of OFDM waveforms in the presence of receiver RF impairments," in *IEEE Wireless Communications and Networking Conference (WCNC)*, Apr. 2010, pp. 1–6.
- [23] Y. Zhou and Z. Pan, "Impact of LPF mismatch on I/Q imbalance in direct conversion receivers," *IEEE Trans. Wireless Commun.*, vol. 10, no. 6, pp. 1702–1708, Jun. 2011.
- [24] J. Qi, S. Aissa, and M.-S. Alouini, "Dual-hop amplify-and-forward cooperative relaying in the presence of Tx and Rx in-phase and quadrature-phase imbalance," *IET Commun.*, vol. 8, no. 3, pp. 287–298, Feb. 2014.
- [25] J. Li, M. Matthaiou, and T. Svensson, "I/Q imbalance in AF dual-hop relaying: Performance analysis in Nakagami- m fading," *IEEE Trans. Commun.*, vol. 62, no. 3, pp. 836–847, Mar. 2014.
- [26] M. Mokhtar, A.-A. A. Boulogeorgos, G. K. Karagiannidis, and N. Al-Dhahir, "OFDM opportunistic relaying under joint transmit/receive I/Q imbalance," *IEEE Trans. Commun.*, vol. 62, no. 5, pp. 1458–1468, May 2014.
- [27] J. Li, M. Matthaiou, and T. Svensson, "I/Q imbalance in two-way AF relaying," *IEEE Trans. Commun.*, vol. 62, no. 7, pp. 2271–2285, Jul. 2014.
- [28] E. Bjornson, A. Papadogiannis, M. Matthaiou, and M. Debbah, "On the impact of transceiver impairments on AF relaying," in *Proc. IEEE International Conference on Acoustics, Speech and Signal Processing (ICASSP)*, May 2013.
- [29] E. Bjornson, M. Matthaiou, and M. Debbah, "Massive MIMO systems with hardware-constrained base stations," in *IEEE International Conference on Acoustics, Speech and Signal Processing (ICASSP)*, May 2014, pp. 3142–3146.
- [30] Q. Zou, A. Tarighat, and A. Sayed, "Joint compensation of IQ imbalance and phase noise in OFDM wireless systems," *IEEE Transactions on Communications*, vol. 57, no. 2, pp. 404–414, Feb. 2009.

- [31] M. Grimm, M. Allen, J. Marttila, M. Valkama, and R. Thoma, "Joint mitigation of nonlinear RF and baseband distortions in wideband direct-conversion receivers," *IEEE Trans. Microw. Theory Tech.*, vol. 62, no. 1, pp. 166–182, Jan. 2014.
- [32] S. Heinen and R. Wunderlich, "High dynamic range RF frontends from multiband multistandard to cognitive radio," in *Semiconductor Conference Dresden (SCD)*, Sep. 2011, pp. 1–8.
- [33] D. Cabric, S. Mishra, and R. Brodersen, "Implementation issues in spectrum sensing for cognitive radios," in *Conference Record of the Thirty-Eighth Asilomar Conference on Signals, Systems and Computers*, vol. 1, Nov. 2004, pp. 772–776.
- [34] A. ElSamadouny, A. Gomaa, and N. Al-Dhahir, "Likelihood-based spectrum sensing of OFDM signals in the presence of Tx/Rx I/Q imbalance," in *IEEE Global Communications Conference (GLOBECOM)*, Dec. 2012, pp. 3616–3621.
- [35] O. Semiari, B. Maham, and C. Yuen, "Effect of I/Q imbalance on blind spectrum sensing for OFDMA overlay cognitive radio," in *1st IEEE International Conference on Communications in China (ICCC)*, Aug. 2012, pp. 433–437.
- [36] E. Rebeiz, A. Ghadam, M. Valkama, and D. Cabric, "Spectrum sensing under RF non-linearities: Performance analysis and DSP-enhanced receivers," *IEEE Trans. Signal Process.*, vol. 63, no. 8, pp. 1950–1964, Apr. 2015.
- [37] I. S. Gradshteyn and I. M. Ryzhik, *Table of Integrals, Series, and Products*, 6th ed. New York: Academic, 2000.
- [38] A. Chaudhry and S. Zubair, *On a Class of Incomplete Gamma Functions with Applications*. CRC Press, 2001.
- [39] S. Mirabbasi and K. Martin, "Classical and modern receiver architectures," *IEEE Commun. Mag.*, vol. 38, no. 11, pp. 132–139, Nov. 2000.
- [40] C. Studer, M. Wenk, and A. Burg, "MIMO transmission with residual transmit-RF impairments," in *International ITG Workshop on Smart Antennas (WSA)*, Feb. 2010, pp. 189–196.
- [41] D. Dardari, V. Tralli, and A. Vaccari, "A theoretical characterization of nonlinear distortion effects in OFDM systems," *IEEE Trans. Commun.*, vol. 48, no. 10, pp. 1755–1764, Oct. 2000.
- [42] E. Bjornson, A. Papadogiannis, M. Matthaiou, and M. Debbah, "On the impact of transceiver impairments on AF relaying," in *IEEE International Conference on Acoustics, Speech and Signal Processing (ICASSP)*, May 2013, pp. 4948–4952.
- [43] P. Zetterberg, "Experimental investigation of TDD reciprocity-based zero-forcing transmit precoding," *EURASIP Journal on Advances in Signal Processing*, vol. 2011, no. 1, p. 137541, 2011.
- [44] A. Papoulis and S. Pillai, *Probability, Random Variables, and Stochastic Processes*, ser. McGraw-Hill series in electrical engineering: Communications and signal processing. Tata McGraw-Hill, 2002.
- [45] A.-A. A. Boulogeorgos, P. C. Sofotasios, S. Muhaidat, M. Valkama, and G. K. Karagiannidis, "The effects of RF impairments in Vehicle-to-Vehicle communications," in *IEEE 25th International Symposium on Personal, Indoor and Mobile Radio Communications - (PIMRC): Fundamentals and PHY (IEEE PIMRC 2015 - Fundamentals and PHY)*, Hong Kong, P.R. China, Aug. 2015.
- [46] G. K. Karagiannidis, N. C. Sagias, and T. A. Tsiftsis, "Closed-form statistics for the sum of squared Nakagami-m variates and its applications," *IEEE Trans. Commun.*, vol. 54, pp. 1353–1359, Aug. 2006.
- [47] M. Abramowitz and I. A. Stegun, *Handbook of Mathematical Functions with Formulas, Graphs, and Mathematical Tables*. New York: Dover Publications, 1965.